Investigation of the mode splitting induced by electro-optic birefringence in a vertical-cavity surface-emitting laser by polarized electroluminescence*

Zhang Jie(章 杰)[a], Yu Jin-Ling(俞金玲)[a]†, Cheng Shu-Ying(程树英)[a], Lai Yun-Feng(赖云锋)[a], and Chen Yong-Hai(陈涌海)[b]‡

[a] College of Physics and Information Engineering, and Institute of Micro/Nano Devices and Solar Cells, Fuzhou University, Fuzhou 350108, China
[b] Key Laboratory of Semiconductor Materials Science, Institute of Semiconductors, Chinese Academy of Sciences, Beijing 100083, China

(Received 3 May 2013; revised manuscript received 17 July 2013; published online 20 December 2013)

The mode splitting induced by electro-optic birefringence in a P–I–N InGaAs/GaAs/AlGaAs vertical-cavity surface-emitting laser (VCSEL) has been studied by polarized electroluminescence (EL) at room temperature. The polarized EL spectra with $E \parallel [110]$ and $E \parallel [1\bar{1}0]$ directions, are extracted for different injected currents. The mode splitting of the two orthogonal polarized modes for a VCSEL device is determined, and its value increases linearly with the increasing injected current due to electro-optic birefringence. This article demonstrates that the polarized EL is a powerful tool to study the mode splitting and polarization anisotropy of a VCSEL device.

Keywords: mode splitting, electro-optic birefringence, vertical-cavity surface-emitting laser, polarized electroluminescence

PACS: 73.21.Fg, 78.40.Fy, 78.67.De **DOI:** 10.1088/1674-1056/23/2/027304

1. Introduction

The vertical-cavity surface-emitting laser (VCSEL) has many advantages compared to an edge-emitting laser, such as low threshold currents, two-dimensional array operation, single mode operation and circular spot profiles of the output light.[1] Therefore it has attracted much research interest in recent decades.[1–9] A VCSEL device usually emits two orthogonally polarized lights along two specific crystal directions, such as [110] and $[1\bar{1}0]$ directions for (001) GaAs-based VCSELs. For an ideal rotationally symmetric VCSEL device with a high degree of in-plane isotropy, these two transverse modes are degenerate. However, the unavoidable residual stress, internal electric field or the noncircular shape of the VCSEL will break the symmetry, and introduce birefringence into the structure. The birefringence will lift the polarization degeneracy and result in a frequency splitting of the two polarization modes. Thus, the cavity resonances in the [110] and $[1\bar{1}0]$ directions are different. It is reported that the value of the mode splitting plays an important role in determining both the mechanism of polarization switching of a VCSEL,[10] and the design of polarization stable devices.[11,12] However, it is very difficult to directly obtain the splitting by spectroscopies, even at much lower temperatures, due to the fact that the birefringence splitting (typically several tens to hundreds of μeV) is much smaller than the inhomogeneous broadening of the linewidth of the spectrum (typically 2 meV–3 meV). Nowadays, there are several techniques which can directly measure the mode splitting of a VCSEL device, for example, planar Fabry–Perot interferometer,[11,12] polarization beat technique,[12] and reflectance difference spectroscopy (RDS).[5] Planar Fabry–Perot interferometer makes use of a large number of interfering rays between two closely spaced partially silvered surfaces to obtain high spectral resolution (about 1 GHz). The polarization beat technique measures the intensity of the noise spectrum of the laser output after a polarizer. If the polarizer is oriented at an angle between the polarization axes of the two modes, a beat peak is observed in the noise spectrum. The frequency of this peak is equal to the frequency splitting between the two modes.[12] Compared to the planar Fabry–Perot interferometer, it has a higher spectral resolution. These two methods can directly measure the mode splitting of a laser, but the measurement system is quite complex. RDS measures the reflectance difference of a VCSEL structure, and then obtains the mode splitting by spectra fitting. Compared to the two methods mentioned above, its advantages are seen in its ability to study the mode splitting of a wafer-scale VCSEL structure. However, its data analysis is more complex. In this paper, we present a new method using polarized electroluminescence (EL) to quantitatively obtain the mode splitting induced by electro-optic birefringence

*Project supported the National Key Basic Research and Development Program of China (Grant Nos. 2012CB921304 and 2013CB632805), the National Natural Science Foundation of China (Grant Nos. 60990313, 61306120, and 6106003), and the Foundation of Fuzhou University (Grant No. 022498).

†Corresponding author. E-mail: JLYU@semi.ac.cn
‡Corresponding author. E-mail: yhchen@semi.ac.cn

© 2014 Chinese Physical Society and IOP Publishing Ltd

in a P–I–N InGaAs/GaAs/AlGaAs VCSEL at room temperature. Compared to the previous methods we mentioned above, it uses more simple equipment and has an easier data analysis approach. In this paper, the polarized EL spectra with $E \parallel [110]$ and $E \parallel [1\bar{1}0]$ directions, respectively, are extracted for different injected currents. Then we obtain the mode splitting of the two orthogonal polarized modes for a VCSEL device under different injected currents, and we find that the mode splitting changes linearly with the injected current due to electro-optic birefringence.

2. Model and method

The VCSEL studied here consists of three 7.5-nm-thick InGaAs quantum wells (QWs) centered in a 1λ cavity of $Al_xGa_{1-x}As$ graded structure, with the *p*-doped top and *n*-doped bottom distributed bragg reflectors (DBR) formed with alternating graded layers of 31 and 25 pairs of $Al_xGa_{1-x}As/Al_yGa_{1-y}As$ ($x = 0.9$–0.15, $y = 0.15$–0.9) quarter-wave stacks, respectively. The *p* contact is made by depositing Au/Zn, and the *n* contact is made of a Au/Ge/Ni/Au metal multilayer structure. The air-posed VCSEL device is bottom-emitting with a central aperture of 400 μm for the laser emission. The *L–I–V* characteristics of the VCSEL device are shown in Fig. 1.

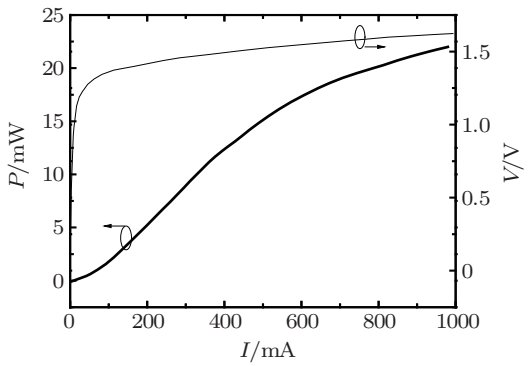


Fig. 1. The *L–I–V* characteristics of the VCSEL device.

The setup of the polarized EL system is shown in Fig. 2. In this system, light emitted from the VCSEL device goes through a convex lens to become a quasi-parallel beam, and then it goes through another convex lens to be focused on the slit of the monochromator, as shown in Fig. 2. Then the light goes through a photoelastic modulator (PEM), a polarizer, a monochromator, and is finally detected by an InGaAs photoelectric detector. The optical axial of the PEM is rotated by an angle of 45° in the *x*–*y* plane and the transmission axis of the polarizer is parallel to the *x* direction. Here *x* is parallel to the $[1\bar{1}0]$ crystallographic orientation. The spectral resolution is about 1 nm (FWHM). In order to study the influence of the electro-optic effect on the mode splitting, we introduce a pulse current with a repetition rate of 1 kHz and with a duty cycle of 3% flowing along [001] direction.

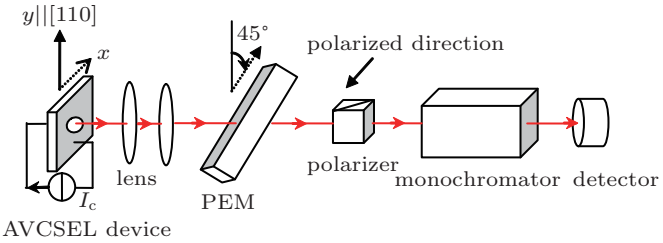


Fig. 2. (color online) A schematic drawing of the polarized EL system.

By using the Mueller matrix approach,[13] the intensity detected by the detector can be written as

$$I = \frac{\pi}{2}(I_{[110]} + I_{[1\bar{1}0]}) + \frac{\pi}{4}(I_{[110]} - I_{[1\bar{1}0]})\mathrm{J}_0(\phi_0), \qquad (1)$$

where $I_{[110]}$ ($I_{[1\bar{1}0]}$) is the intensity of the light polarized along [110] ($[1\bar{1}0]$) crystallographic orientation emitted from the VCSEL device, J_0 is a zero-order Bessel function, and ϕ_0 is the phase retardation introduced by the PEM. If we turn off the PEM, ϕ_0 equals zero, and $\mathrm{J}_0(0)$=1; while if we turn on the PEM and set

$$\phi_0 = 0.5 \times 2\pi, \qquad \mathrm{J}_0(\phi_0) = -0.304.$$

Denoting the intensity detected by the detector as I_{off} and I_{on} when ϕ equals 0 and $0.5 \times 2\pi$, respectively, and according to Eq. (1), we have

$$I_{[110]} = 0.5624 \times I_{\mathrm{off}} - 0.2441 \times I_{\mathrm{on}}, \qquad (2)$$

$$I_{[1\bar{1}0]} = -0.4139 \times I_{\mathrm{off}} + 0.7322 \times I_{\mathrm{on}}. \qquad (3)$$

Thus, we can extract the polarized EL spectra $I_{[110]}$ and $I_{[1\bar{1}0]}$ from the experimentally measured EL signal I_{on} and I_{off} according to Eqs. (2) and (3). By changing the injected current, we can obtain the polarized EL spectra $I_{[110]}$ and $I_{[1\bar{1}0]}$ under different injected currents, and finally obtain the mode splitting due to electro-optic birefringence of the VCSEL device under different injected currents.

3. Results and discussion

Figure 3 shows the EL spectra when PEM is on with ϕ=$0.5 \times 2\pi$ and off with $\phi = 0$, respectively, under injected current of (a) 800 mA, (b) 600 mA, (c) 500 mA, and (d) 400 mA. Then using Eqs. (2) and (3), we can obtain the polarized EL spectra $I_{[110]}$ and $I_{[1\bar{1}0]}$ under different injected currents from the experimentally measured EL spectra I_{on} and I_{off}, as shown in Fig. 4.

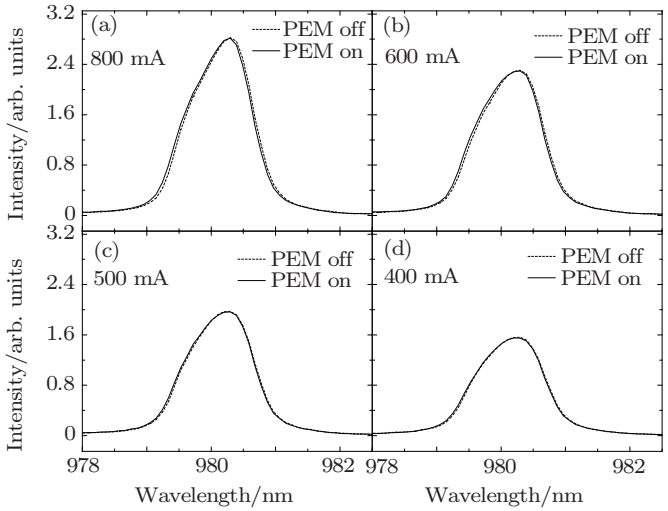


Fig. 3. The EL spectra when PEM is on (solid lines) with $\phi = 0.5 \times 2\pi$ and off (dashed lines) with $\phi = 0$, respectively, under injected current of (a) 800 mA, (b) 600 mA, (c) 500 mA, and (d) 400 mA.

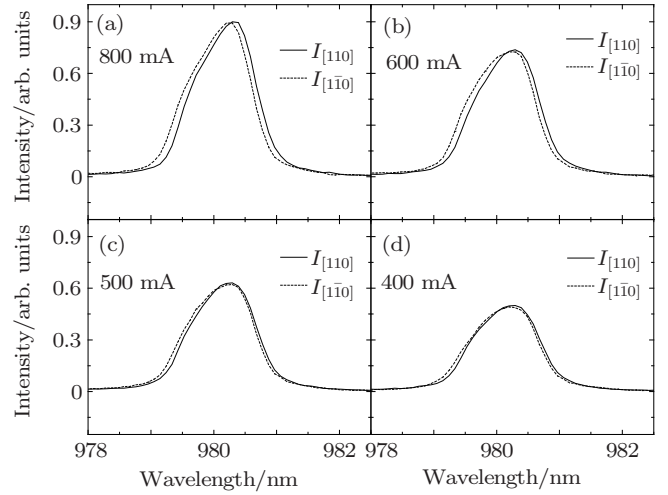


Fig. 4. The polarized EL spectra $I_{[110]}$ (solid lines) and $I_{[1\bar{1}0]}$ (dashed lines) under injected current of (a) 800 mA, (b) 600 mA, (c) 500 mA, and (d) 400 mA extracted from Fig. 3 using Eqs. (2) and (3).

It can be seen that there is an energy difference, i.e. mode splitting, between these two orthogonally polarized modes, and the mode polarized along [110] direction locates at a longer wavelength side than that polarized along $[1\bar{1}0]$ direction. From Fig. 4 we can easily obtain the mode splitting $\Delta E = E_{[110]} - E_{[1\bar{1}0]}$ of the VCSEL device under different injected currents, which is shown in Fig. 5. The solid circles are the experimental results and the line is the linear fitting result. It can be seen that the absolute value of the anisotropic mode splitting ΔE (or $\Delta\nu$) increases linearly with the increasing injected current at a slope of 0.042 GHz/mA. Specifically speaking, when the injected current is increased from 400 mA to 800 mA, the mode splitting is changed from -10.2 GHz to -26.5 GHz nearly linearly. This can be attributed to the linear electric-optic effect, i.e. when an electric field E is applied along [001] direction, the refractive index along [110] and $[1\bar{1}0]$ directions $n_{[110]}$ and $n_{[1\bar{1}0]}$ can be expressed by the following equations[3]

$$n_{[110]} = n_0 - \frac{n_0^3}{2} rE,$$
$$n_{[1\bar{1}0]} = n_0 + \frac{n_0^3}{2} rE. \tag{4}$$

Here n_0 is the refractive index without an electric field, and r is the electro-optic coefficient of $Al_xGa_{1-x}As$. From Eq. (4) we can see that the birefringence of the material shows linear dependence on the electric field. As a result, the mode splitting induced by the birefringence changes linearly with the applied electric field. The mode splitting observed in this experiment is in reasonable agreement with that observed in a commercial proton implanted 780-nm AlGaAs QW VCSEL device (3 GHz–22 GHz) measured by high-resolution spectral measurements reported in Ref. [14]. The minor difference in ΔE between our result and that reported in Ref. [14] may be attributed to the difference of the structure of the devices, since the value of the mode splitting depends on the structure of the VCSEL device and will vary from sample to sample. In our previous works, we studied the uniaxial strain dependence (Ref. [5]) and the temperature dependence (Ref. [15]) of the mode splitting induced by birefringence in an InGaAs/GaAs/AlGaAs VCSEL structure. We found that the mode splitting of the two VCSEL samples was -5.8 GHz and -10 GHz at room temperature without external strain. The small difference in these two values may be due to the fact that in different positions of the wafer, the residual stresses are different, which finally result in different birefringences. It is worth noting that the mode splitting measured by RDS in our previous works were carried out in wafer-scale VCSEL structures, while in this work, the mode splitting is measured in a VCSEL device. Since the preparing process of the device will introduce additional strain, it is reasonable that the mode splitting presented in the device is different from that presented in the wafer.

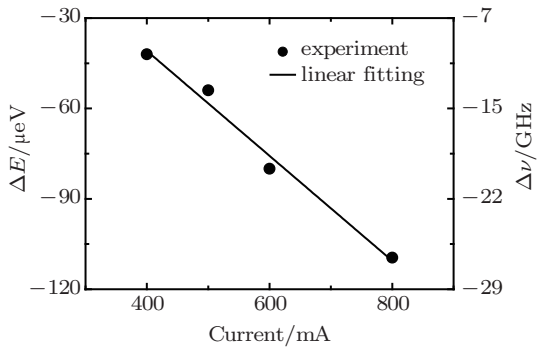


Fig. 5. The mode splitting of the VCSEL device as a function of injected current extracted from Fig. 4. The solid circles are the experimental data, and the solid line is the linear fitting result.

4. Conclusions

In conclusion, we have presented a new method using polarized EL to quantitatively obtain the mode splitting induced by electro-optic birefringence in a P–I–N InGaAs/GaAs/AlGaAs VCSEL at room temperature. The polarized EL spectra with $E \parallel [110]$ and $E \parallel [1\bar{1}0]$ directions under different injected currents are extracted, respectively. Then the mode splitting between the two orthogonally polarized modes under different injected currents is determined. It is found that the mode splitting changes linearly with the injected current, which can be attributed to electro-optic birefringence. We demonstrate that the polarized EL is a powerful tool to study the mode splitting and polarization anisotropy of a VCSEL device.

References

[1] Chavezpirson A, Ando H, Saito H and Kanbe H 1993 *Appl. Phys. Lett.* **62** 3082

[2] Jaeger A, Petroff P M and Lowes T D 2001 *Appl. Phys. Lett.* **78** 3012

[3] Park M S, Ahn B T, Yoo B S, Chu H Y, Park H H and Chang-Hasnain C J 2000 *Appl. Phys. Lett.* **76** 813

[4] Sondermann M, Weinkath M and Ackemann T 2004 *IEEE J. Quantum Electron.* **40** 97

[5] Yu J L, Chen Y H, Jiang C Y, Ye X L and Zhang H Y 2012 *J. Appl. Phys.* **111** 043109

[6] Sondermann M, Weinkath M, Ackemann T, Mulet J and Balle S 2003 *Phys. Rev. A* **68** 033822

[7] Huang M, Wu J, Cui H Y, Qian J Q and Ning Y Q 2012 *Chin. Phys. B* **21** 104207

[8] Shi G Z, Guan B L, Li S and Wang Q 2013 *Chin. Phys. B* **22** 014206

[9] Zhang W L, Pan W, Luo B, Li X F, Zou X H and Wang M Y 2007 *Chin. Phys.* **16** 1996

[10] Balle S, Tolkachova E, San Miguel M, Tredicce J R, Martin-Regalado J and Gahl A 1999 *Opt. Lett.* **24** 1121

[11] Choquette K D, Schneider R P, Lear K L and Leibenguth R E 1995 *IEEE J. Selected Topics in Quantum Electron.* **1** 661

[12] Hendriks R F M, vanExter M P, Woerdman J P, van Geelen A, Weegels L, Gulden K H and Moser M 1997 *Appl. Phys. Lett.* **71** 2599

[13] Hiroyuki F 2007 *Spectroscopic Ellipsometry* (Chichester: John Wiley and Sons, Ltd) pp. 60–78

[14] Vandoorn A K J, Vanexter M P and Woerdman J P 1994 *Electron. Lett.* **30** 1941

[15] Yu J L, Chen Y H, Cheng S Y and Lai Y F 2013 *Appl. Opt.* **52** 1035